

The effect of phase fluctuations on the single-particle properties of the underdoped cuprates

Hyok-Jon Kwon* and Alan T. Dorsey**

Department of Physics, University of Florida, Gainesville, FL 32611-8440

(September 16, 1998)

We study the effect of order parameter phase fluctuations on the single-particle properties of fermions in the underdoped cuprate superconductors using a phenomenological low-energy theory. We identify the fermion-phase field coupling as the Doppler-shift of the quasiparticle spectrum induced by the fluctuating superfluid velocity and we calculate the effect of these fluctuations on the fermion self-energy. We show that the vortex pair unbinding near the superconducting transition causes a significant broadening in the fermion spectral function, producing a pseudogap-like feature. We also discuss the specific heat and show that the phase fluctuation effect is visible due to the short coherence length.

PACS numbers: 74.20.-z, 74.25.-q, 74.40.+k, 74.72.-h

I. INTRODUCTION

One of the more intriguing properties of the cuprate superconductors is the existence of a “pseudogap” regime in the normal phase, which develops when these materials are underdoped and at temperatures below a characteristic temperature T^* (see Fig. 1). Numerous experiments, including NMR,¹ neutron scattering,² infrared and optical conductivity,³ transport,⁴ Raman scattering,⁵ specific heat,⁶ angle-resolved photoemission (ARPES),⁷ and scanning tunneling spectroscopy (STS),⁸ indicate that in this regime there is a gap in the excitation spectrum, while transport measurements show that the sample is normal and that the superfluid density is zero.⁹ The ARPES and STS experiments on $\text{Bi}_2\text{Sr}_2\text{CaCu}_2\text{O}_{8+\delta}$ have established that the pseudogap evolves smoothly from the superconducting gap. More significantly, the ARPES results show that the pseudogap in the normal phase possesses the same $d_{x^2-y^2}$ symmetry as the superconducting gap; the node along the $(\pi/2, \pi/2)$ direction in the superconducting phase evolves into an extended gapless region with increasing temperature in the pseudogap regime, while the gap maximum in the $(\pi, 0)$ direction has only a very weak temperature dependence. Taken collectively, these results demonstrate that the pseudogap in the normal phase is a remnant of the quasiparticle gap in the superconducting phase.

The theoretical challenge in understanding the pseudogap regime is then to reconcile the existence of a quasiparticle gap with the absence of superconducting order. The usual strategy in studying superconductivity is to start from a normal phase consisting of well-defined Landau quasiparticles and to then ask what interactions lead to a superconducting instability. Here, the experiments suggest that we start from the *superconducting* phase—skirting the issue of the origin of the pairing—and ask what mechanisms would destroy phase coherence while

preserving the gap in the excitation spectrum.

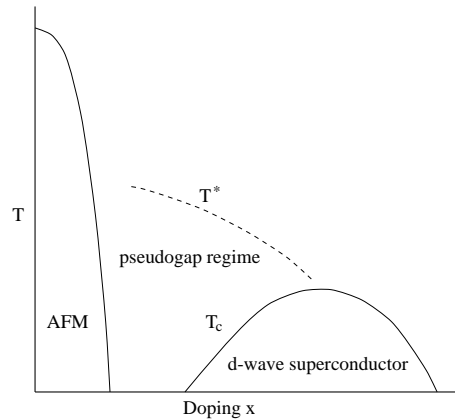


FIG. 1. Schematic phase diagram of a cuprate superconductor as a function of temperature T and doping x . AFM denotes the antiferromagnetic insulating phase.

The mechanism which we explore in this paper, originally suggested by Emery and Kivelson,¹⁰ is that the local superconducting order parameter $\Delta(\mathbf{x}) = \Delta_0 e^{i\theta(\mathbf{x})}$ has a well defined amplitude Δ_0 (set by energies of order T^*) but a fluctuating phase θ , such that $\langle \Delta(\mathbf{x}) \rangle = \Delta_0 \langle e^{i\theta(\mathbf{x})} \rangle = 0$ in the pseudogap regime. The temperature scale for phase fluctuations T^{phase} is controlled by the zero-temperature superfluid stiffness $n_s(0)/4m$; the actual critical temperature $T_c = \min\{T^{\text{phase}}, T^{\text{MF}}\}$, with T^{MF} the mean-field transition temperature predicted in BCS theory. Emery and Kivelson argued that in conventional low- T_c superconductors, which have a large superfluid stiffness, $T^{\text{phase}} \gg T_c$, so that phase fluctuations are irrelevant and the transition is BCS-like. However, cuprate superconductors are doped Mott insulators which have a small superfluid stiffness (of order the doping x), so that $T^{\text{phase}} \sim T_c$ and the transition is con-

trolled by phase ordering. This naturally explains the Uemura scaling,¹¹ $T_c \sim n_s(0)/m$, observed in the cuprate superconductors. In addition, the reduction of the phase-stiffness $n_s(T)/4m$ is approximately linear in temperature due to the d -wave symmetry, almost all the way to T_c ,¹² in contrast to conventional s -wave superconductors, where $n_s(T)/4m$ rapidly drops to zero near T_c .¹³ Therefore the temperature range for which $n_s(T)/4m$ is a small number is much wider than in the conventional superconductors, and the effect of phase fluctuations can be observed even far from T_c .

In this paper we investigate the effects of phase fluctuations on the fermion single-particle properties and the thermodynamics near the superconducting transition, without regard to the details of a microscopic model. In addition to the smallness of $n_s(T)/4m$, we assume that the superconducting gap and the normal state pseudogap have a d -wave symmetry and that the system is two-dimensional due to the weakness of the interlayer coupling. We find that phase fluctuations, and in particular transverse phase fluctuations, can have a pronounced effect on the spectral function, density of states, and specific heat near the transition.

A brief overview of the paper is as follows: In Sec. II we construct a low-energy effective theory of fermion quasiparticles coupled to the classical phase fluctuations by integrating out the fast momentum degrees of freedom. In Sec. III we obtain the self-energy of the (neutral) fermion quasiparticles and calculate the single-particle density of states and the spectral broadening. We observe that the peak in the spectral function and the density of states near the gap is significantly broadened by the phase fluctuations (vortex pair unbinding) near the transition temperature, exhibiting a pseudogap-like behavior. In Sec. IV we consider the effect of the phase fluctuations on the specific heat near the transition. We find that the vortex-antivortex unbinding transition causes a visible peak in the specific heat just above the transition temperature due to the short coherence length of the materials. Appendix A is a compilation of some useful results on the Berezinskii-Kosterlitz-Thouless transition, and Appendix B contains some technical details on the calculation of the fermion self-energy.

II. EFFECTIVE LOW-ENERGY THEORY

In this section we derive a low-energy effective theory of fermion quasiparticles coupled to the phase fluctuations of the superconducting order parameter, assuming that the amplitude fluctuations are negligible near T_c . For simplicity, we consider an s -wave symmetry of the gap in this section. Extensions to other gap symmetries are straightforward.

We begin with the mean-field BCS model whose partition function is given by

$$Z = \int \mathcal{D}c_\sigma \mathcal{D}c_\sigma^\dagger \mathcal{D}\Delta \mathcal{D}\Delta^* e^{-S}, \quad (2.1)$$

where

$$S = \int d^2x \int_0^\beta d\tau \left[\sum_\sigma c_\sigma^\dagger(\mathbf{x}, \tau) \left(\partial_\tau - \frac{\nabla^2}{2m_0} - \mu \right) c_\sigma(\mathbf{x}, \tau) + \Delta(\mathbf{x}, \tau) c_\uparrow^\dagger(\mathbf{x}, \tau) c_\downarrow^\dagger(\mathbf{x}, \tau) + \text{h.c.} + \frac{1}{g} |\Delta(\mathbf{x}, \tau)|^2 \right], \quad (2.2)$$

with the interaction strength $g > 0$. The pairing field $\Delta(\mathbf{x}, \tau) = |\Delta(\mathbf{x}, \tau)| e^{i\theta(\mathbf{x}, \tau)}$; in what follows we will assume that the amplitude of the order parameter is constant, $|\Delta(\mathbf{x}, \tau)| = \Delta$, and concentrate on the phase degree of freedom, θ . Also we have not considered the effect of Coulomb interactions. In order to couple the fermions to the θ field more explicitly, we perform a gauge transformation $\psi_\sigma(\mathbf{x}, \tau) = c_\sigma(\mathbf{x}, \tau) e^{-i\theta(\mathbf{x}, \tau)/2}$, with ψ_σ the field operators for neutral fermions.¹⁴ Then we obtain a new action for the neutral fermions as

$$S = \int d^2x \int_0^\beta d\tau \left\{ \sum_\sigma \psi_\sigma^\dagger(\mathbf{x}, \tau) \left[(\partial_\tau + i\partial_\tau\theta/2) - \frac{(\nabla + i\nabla\theta/2)^2}{2m_0} - \mu \right] \psi_\sigma(\mathbf{x}, \tau) + \Delta \psi_\uparrow^\dagger(\mathbf{x}, \tau) \psi_\downarrow^\dagger(\mathbf{x}, \tau) + \text{h.c.} + \frac{1}{g} \Delta^2 \right\}. \quad (2.3)$$

The last term in Eq. (2.3) is a constant and will be dropped in what follows.

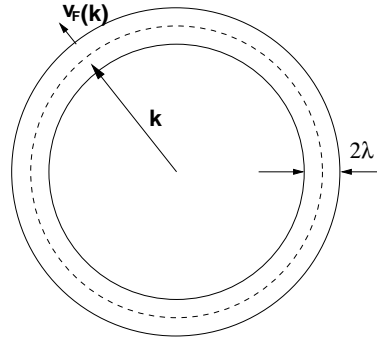


FIG. 2. Hilbert space of the low-energy effective theory. After the inner and outer side of the thin momentum shell degree of freedom has been integrated out, we are left with a theory of fermion quasiparticles living in a thin momentum shell of thickness 2λ . The dashed line denotes the Fermi surface. The direction of the Fermi velocity $\mathbf{v}_F(\mathbf{k})$ is in parallel with the momentum \mathbf{k} of the fermion quasiparticle $\psi(\mathbf{k})$.

As it stands, Eq. (2.3) is hard to study, so we integrate out the fast momentum degrees of freedom and focus on the low-energy properties of the system.¹⁵ Namely, $\psi \rightarrow \psi + \psi'$ where $\psi'(\mathbf{x}) = \sum_{||\mathbf{k}|-k_F|>\lambda} \psi_{\mathbf{k}} e^{i\mathbf{k}\cdot\mathbf{x}}$ is the fast momentum degree of freedom which is to be integrated out

of the partition function and $\psi(\mathbf{x}) = \sum_{||\mathbf{k}|-k_F|<\lambda} \psi_{\mathbf{k}} e^{i\mathbf{k}\cdot\mathbf{x}}$ is the low-energy quasiparticle. Then

$$\begin{aligned} \mathcal{Z} &= \int \mathcal{D}\psi' \mathcal{D}\psi'^{\dagger} \mathcal{D}\psi \mathcal{D}\psi^{\dagger} \mathcal{D}\theta e^{-S} \\ &= \mathcal{N} \int \mathcal{D}\psi \mathcal{D}\psi^{\dagger} \mathcal{D}\theta e^{-S_{\text{eff}}}, \end{aligned} \quad (2.4)$$

and we are left with the momentum degrees of freedom in the vicinity of the Fermi surface if we take $\lambda \ll k_F$. Since we will be considering the effect of fluctuating vortices on the fermion self-energy, and the characteristic vortex core size is of order the coherence length ξ_0 , we will take λ of order $1/\xi_0$. We are therefore working in the limit $k_F \xi_0 \gg 1$; in the cuprates it is estimated that $k_F \xi_0 \sim 10$,¹⁶ so our approximation is appropriate for these materials.

The effective action of the fermions near the Fermi surface and the phase field is

$$\begin{aligned} S_{\text{eff}} &= \sum_{\sigma} \left[T \sum_{\mathbf{k}, \omega} \psi_{\sigma}^{\dagger}(\mathbf{k}, \omega) \psi_{\sigma}(\mathbf{k}, \omega) (i\omega - k^2/2m + \mu) \right. \\ &\quad + \int d^2x \int_0^{\beta} d\tau \psi_{\sigma}^{\dagger}(\mathbf{x}, \tau) (i\partial_{\tau} \theta / 2 \\ &\quad \left. - \frac{i}{2m} \nabla \theta \cdot \nabla) \psi_{\sigma}(\mathbf{x}, \tau) \right] \\ &\quad + \frac{1}{2} T \sum_{\mathbf{q}, \nu} \frac{n_f}{4m} \mathbf{q}^2 \theta(\mathbf{q}, \nu) \theta(-\mathbf{q}, -\nu) \\ &\quad + T \sum_{\mathbf{k}, \omega} \Delta \psi_{\uparrow}^{\dagger}(\mathbf{k}, \omega) \psi_{\downarrow}^{\dagger}(-\mathbf{k}, -\omega) + \text{h.c.} \end{aligned} \quad (2.5)$$

Here we have neglected higher orders in $q/k \ll 1$ since $k \approx k_F$ and $|\mathbf{q}| < \lambda$, and we have taken $c_{\sigma}^{\dagger} c_{\sigma} \approx n_f$, the total number of fermions. Since \mathbf{k} is close to the Fermi surface, we may linearize the fermionic spectrum as $k^2/2m - \mu \equiv \xi_{\mathbf{k}} \approx v_F(|\mathbf{k}| - k_F)$. The resulting effective action is expressed in terms of the Nambu spinor notation, $\hat{\psi} = (\psi_{\uparrow}, \psi_{\downarrow}^{\dagger})$, as

$$S_{\text{eff}} = S_0 + S_I, \quad (2.6)$$

with

$$\begin{aligned} S_0 &= T \sum_{\mathbf{k}, \omega} \hat{\psi}^{\dagger} \hat{G}_0^{-1} \hat{\psi} \\ &\quad + \frac{1}{2} \int_0^{\beta} d\tau \int d^2x \frac{n_f}{4m} [\nabla \theta(\mathbf{x}, \tau)]^2 \end{aligned} \quad (2.7)$$

and

$$\begin{aligned} S_I &= \int d^2x \int_0^{\beta} d\tau \hat{\psi}^{\dagger}(\mathbf{x}, \tau) \left(i\partial_{\tau} \theta / 2 \right. \\ &\quad \left. - \frac{i}{2m} \nabla \theta \cdot \nabla \right) \hat{\psi}(\mathbf{x}, \tau). \end{aligned} \quad (2.8)$$

Here

$$\hat{G}_0^{-1} = \begin{pmatrix} i\omega - \xi_{\mathbf{k}} & -\Delta \\ -\Delta & i\omega + \xi_{\mathbf{k}} \end{pmatrix}, \quad (2.9)$$

with \hat{G}_0 the bare Green's function for the neutral fermions,

$$\hat{G}_0 = \begin{pmatrix} \mathcal{G}_0(\mathbf{k}, \omega) & \mathcal{F}_0(\mathbf{k}, \omega) \\ \mathcal{F}_0(\mathbf{k}, \omega) & -\mathcal{G}_0(\mathbf{k}, -\omega) \end{pmatrix}, \quad (2.10)$$

$$\begin{aligned} \mathcal{G}_0(\mathbf{k}, \omega) &= \frac{i\omega + \xi_{\mathbf{k}}}{(i\omega - \xi_{\mathbf{k}})(i\omega + \xi_{\mathbf{k}}) - \Delta^2}, \\ \mathcal{F}_0(\mathbf{k}, \omega) &= \frac{\Delta}{(i\omega - \xi_{\mathbf{k}})(i\omega + \xi_{\mathbf{k}}) - \Delta^2}. \end{aligned} \quad (2.11)$$

The microscopic physics relevant to the length scale $L < \xi_0$ (the vortex core structure, for instance) has been integrated out to renormalize such quantities as the effective mass m and the residual interactions between the quasiparticles which we have not included here. Therefore, in this effective theory the vortices are treated as point-like entities.

In studying the finite temperature superconductor to normal metal transition, it should be sufficient to consider only the static fluctuations of the phase, and we may suppress the time-dependence in θ and retain only the spatial fluctuation. The interaction term is then reduced to

$$S_I = -T \sum_{\mathbf{k}, \mathbf{q}, \omega} m \mathbf{v}_F(\mathbf{k}) \cdot \mathbf{v}_s(\mathbf{q}) \hat{\psi}^{\dagger}(\mathbf{k} + \mathbf{q}, \omega) \hat{\psi}(\mathbf{k}, \omega). \quad (2.12)$$

Here we take $\mathbf{k}/m \approx \mathbf{v}_F(\mathbf{k})$ where $\mathbf{v}_F(\mathbf{k})$ is the Fermi velocity at the Fermi surface point closest to the wave vector \mathbf{k} (see Fig. 2), and $\mathbf{v}_s(\mathbf{q}) = \int d^2x e^{-i\mathbf{q}\cdot\mathbf{x}} \nabla \theta(\mathbf{x}) / 2m$ is the superfluid velocity. One should bear in mind that $\mathbf{v}_s(\mathbf{q})$ includes both longitudinal and transverse components.

When the interaction is expressed in form of Eq. (2.12) we see that S_I is the Doppler shift of the fermion spectrum due to a non-zero superfluid velocity. This becomes more explicit if we consider the $q \rightarrow 0$ limit of S_I , neglecting the \mathbf{q} dependence of the field operators, so that the superfluid velocity can be subsumed into the fermion Green's function as

$$\hat{G}^{-1} = \begin{pmatrix} i\omega - \xi_{\mathbf{k}} - \mathbf{p}_F \cdot \mathbf{v}_s & -\Delta \\ -\Delta & i\omega + \xi_{\mathbf{k}} - \mathbf{p}_F \cdot \mathbf{v}_s \end{pmatrix}, \quad (2.13)$$

where $\mathbf{p}_F \equiv m \mathbf{v}_F(\mathbf{k})$. A semiclassical approximation of this form has recently been used by Franz and Millis¹⁷ to study phase fluctuations in the underdoped cuprates. They incorporated the phase fluctuations by averaging the Green's function over a Gaussian distribution of velocity fluctuations. Our approach is rather different—we treat the coupling to the fluctuating phase using a self-consistent perturbation theory (see Sec. III) in order to calculate the fermion self-energy due to phase fluctuations.

Finally, we can check if the effective theory correctly gives the effective action of the phase fluctuations¹⁸ by integrating out the remaining fermionic degrees of freedom.

By expanding e^{-S_I} to second order in θ , and integrating out the fermion fields, we obtain

$$S[\theta] \approx \frac{1}{2} \sum_{\mathbf{k}, \mathbf{q}, \omega} \left(\frac{v_F^2 q^2}{4} \right) \text{Tr} \left[\hat{G}_0(\mathbf{k}, \omega) \hat{G}_0(\mathbf{k} + \mathbf{q}, \omega) \right] \\ \times \theta(\mathbf{q}) \theta(-\mathbf{q}) + \frac{1}{2T} \sum_{\mathbf{q}} \frac{n_f}{4m} q^2 \theta(\mathbf{q}) \theta(-\mathbf{q}). \quad (2.14)$$

The superfluid density at temperature T is¹³

$$n_s(T) = n_f + \lim_{\mathbf{q} \rightarrow 0} \lim_{\nu \rightarrow 0} \frac{T}{m} \sum_{\mathbf{k}, \omega} (\mathbf{k} + \mathbf{q}/2)_i (\mathbf{k} + \mathbf{q}/2)_i \\ \times \text{Tr} \left[\hat{G}_0(\mathbf{k}, \omega) \hat{G}_0(\mathbf{k} + \mathbf{q}, \omega + \nu) \right]. \quad (2.15)$$

Therefore, for $|\mathbf{q}| \ll \Delta/v_F$, we recognize that Eq. (2.14) has the following form:

$$S[\theta] \approx \frac{1}{2T} \sum_{\mathbf{q}} \frac{n_s(T)}{4m} q^2 \theta(\mathbf{q}) \theta(-\mathbf{q}). \quad (2.16)$$

We see that the stiffness of the phase fluctuations can be identified as the superfluid density at T . This result holds even when we consider unconventional order parameter symmetry.

Equation (2.16) can serve as a convenient effective theory to describe the critical properties of the Berezinskii-Kosterlitz-Thouless (BKT) transition.¹⁹ The macroscopic measurable quantities are often insensitive to the detailed microscopic fermion theory except through the parameter $n_s(T)/m$, and the effective description of phase fluctuations is enough to characterize the transitions in macroscopic quantities. A brief discussion of the BKT transition and derivation of the effective classical action are included in Appendix A for completeness. We should stress that we are *not* proposing that the superconducting transition in the cuprates is of the BKT type; weak interplanar coupling will produce a transition in the $d = 3$ XY universality class, sufficiently close the transition. However, outside this regime two-dimensional vortex fluctuations will dominate the low-energy physics, and we expect the physics discussed in the subsequent sections to pertain. Indeed, recent time-domain terahertz spectroscopy measurements²⁰ of the complex conductivity $\sigma(\omega)$ of underdoped $\text{Bi}_2\text{Sr}_2\text{CaCu}_2\text{O}_{8+\delta}$, which provide a direct probe of the superfluid density, show that the dynamics is well described by the BKT picture, lending credence to the model developed in this paper.

III. SINGLE-PARTICLE PROPERTIES OF FERMIONS WITH PHASE FLUCTUATIONS

The underdoped cuprate superconductors can be regarded as doped Mott insulators with a small charge carrier density (superfluid density), in other words, $n_s(0)/m \sim xE_F$ where x is the doping concentration.

To calculate the fermionic self-energy, we have to perform a perturbative expansion in θ from Eq. (2.3), but close to T_c and for a small superfluid density, there is no obvious small parameter. We need a way to select a set of meaningful diagrams. The saving grace in this case is that the volume (perimeter) of the Fermi surface is large, so that we can select the diagrams of leading order in $1/N(0)$. One way of keeping track of the diagrams is to introduce n fermion species and perform a $1/n$ expansion and at the end take $n \rightarrow 1$. This amounts to summing over ring diagrams. Other diagrams are smaller by factors of λ/k_F since only the ring diagrams involve summations over the Fermi surface perimeter in this low-energy effective theory. In this section we study the effect of phase fluctuations on the single-particle properties of the fermions using this machinery, both at $T < T_{BKT}$ and $T > T_{BKT}$. For the rest of the paper, we reinstate the angular dependence of the gap function $\Delta(\phi)$, and perform calculations assuming a $d_{x^2-y^2}$ -wave symmetry, $\Delta(\phi) = \Delta_0 \cos 2\phi$, neglecting the temperature dependence in Δ_0 since it changes smoothly through the transition in the underdoped cuprates.



FIG. 3. The propagator of the velocity field in the leading order in λ/k_F . The thin (thick) wiggly line is the bare (full) propagator. The ring in the figure is the polarization of the fermions.

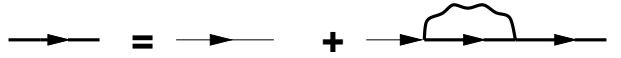


FIG. 4. The Dyson equation of fermion Green's function. The wiggly line is the velocity propagator. The thin (thick) solid line is the bare (full) Green's function.

We first calculate the velocity-velocity correlation function from the effective theory we obtained in Sec. II by summing over the ring diagrams as in Fig. 3. We find that

$$\langle v_s^\alpha(\mathbf{q}) v_s^\beta(-\mathbf{q}) \rangle_{\text{ring}} = \frac{\langle v_s^\alpha(\mathbf{q}) v_s^\beta(-\mathbf{q}) \rangle_0}{1 + \langle v_s^\alpha(\mathbf{q}) v_s^\beta(-\mathbf{q}) \rangle_0 \Pi_{\alpha\beta}(\mathbf{q}, \omega)}, \quad (3.1)$$

where

$$\Pi_{\alpha\beta}(\mathbf{q}, \omega) = \sum_{\mathbf{k}} [m\mathbf{v}_F(\mathbf{k})]_\alpha [m\mathbf{v}_F(\mathbf{k})]_\beta \\ \times \text{Tr} [\hat{G}_0(\mathbf{k} + \mathbf{q}, \omega) \hat{G}_0(\mathbf{k}, \omega)]. \quad (3.2)$$

Now we calculate the fermion self-energy correction from the Dyson equation,

$$\hat{\Sigma}(\mathbf{k}, \omega) = \sum_{\mathbf{q}} [m\mathbf{v}_F(\mathbf{k})]_\alpha [m\mathbf{v}_F(\mathbf{k})]_\beta \\ \times \langle v_s^\alpha(\mathbf{q}) v_s^\beta(-\mathbf{q}) \rangle_{\text{ring}} \hat{G}(\mathbf{k} - \mathbf{q}, \omega), \quad (3.3)$$

where \hat{G} is the full fermion Green's function, given self-consistently by $\hat{G}^{-1} = \hat{G}_0^{-1} - \hat{\Sigma}$. As shown in Appendix A, the velocity-velocity correlation function can be resolved into a longitudinal component $C_l(\mathbf{q})$ and a transverse component $C_t(\mathbf{q})$ [see Eq. (A14)]; as a result, the self energy can be written as a sum of a contribution from longitudinal fluctuations and one from transverse fluctuations,

$$\hat{\Sigma}(\mathbf{k}, \omega) = \hat{\Sigma}_l(\mathbf{k}, \omega) + \hat{\Sigma}_t(\mathbf{k}, \omega), \quad (3.4)$$

where

$$\hat{\Sigma}_l(\mathbf{k}, \omega) = \sum_{\mathbf{q}} [m\mathbf{v}_F(\mathbf{k}) \cdot \hat{q}]^2 C_l(\mathbf{q}) \hat{G}(\mathbf{k} - \mathbf{q}, \omega), \quad (3.5)$$

and

$$\hat{\Sigma}_t(\mathbf{k}, \omega) = \sum_{\mathbf{q}} [m\mathbf{v}_F(\mathbf{k}) \times \hat{q}]^2 C_t(\mathbf{q}) \hat{G}(\mathbf{k} - \mathbf{q}, \omega). \quad (3.6)$$

The self-energy has both a momentum and frequency dependence. Here we focus on the behavior of the self-energy near the Fermi surface, assuming that it varies smoothly near the Fermi surface, and we neglect the $\xi_{\mathbf{k}}$ -dependence. Therefore the only momentum dependence is through the angle ϕ on the Fermi surface.

A. Longitudinal phase fluctuations

First we study the effect of the longitudinal phase fluctuations, neglecting the effect of vortices for now. Using Eqs. (3.5) and (A15), we obtain for the self-energy (see Appendix B for details)

$$\begin{aligned} \hat{\Sigma}_l(\phi, \omega) \approx & \frac{4mT}{n_s(T)} \frac{1}{16\pi} \ln \left[\frac{\lambda^2 + \tilde{\Delta}^2(\phi) + \tilde{\omega}^2}{\tilde{\Delta}^2(\phi) + \tilde{\omega}^2} \right] \\ & \times \begin{pmatrix} -i\tilde{\omega} & -\tilde{\Delta}(\phi) \\ -\tilde{\Delta}(\phi) & -i\tilde{\omega} \end{pmatrix}, \end{aligned} \quad (3.7)$$

where $\tilde{\omega}$ and $\tilde{\Delta}$ can be calculated self-consistently by

$$\begin{pmatrix} i\tilde{\omega} & -\tilde{\Delta}(\phi) \\ -\tilde{\Delta}(\phi) & i\tilde{\omega} \end{pmatrix} = \begin{pmatrix} i\omega & -\Delta(\phi) \\ -\Delta(\phi) & i\omega \end{pmatrix} - \hat{\Sigma}(\phi, \omega). \quad (3.8)$$

By analytically continuing the frequency $i\omega \rightarrow \omega + i\eta$ in Eq. (3.8), we can calculate the single-particle density of states

$$N(\omega) = -\frac{1}{\pi} \text{Im} \int \frac{d\phi}{2\pi} \int d\xi_{\mathbf{k}} \text{Tr} \hat{G}(\mathbf{k}, \omega). \quad (3.9)$$

In order to apply this result to the underdoped cuprates, we need to know the temperature dependence of the superfluid density $n_s(T)$ and the gap $\Delta_0(T)$. We neglect the temperature-dependence of $\Delta_0(T)$, since the

gap smoothly evolves into the pseudogap above T_c . A reasonable form for the superfluid density that approximates the BCS theory is $n_s(T)/4m \approx n_s(0)/4m - \alpha T$ where α is order of unity.²¹ At low temperatures, since the reduction of the superfluid density is approximately linear in temperature, this form is reasonable especially for underdoped cuprates where T_c is relatively low. Throughout this paper we take $\alpha = 3/4$, but the exact value of α is not crucial. Generally the value of α is dependent on the value of Δ_0 .

The curves in Fig. 5 show that the peak in the density of states (DOS) near $\omega = \Delta_0$ is mildly smeared due to the phase fluctuations and the effect is more pronounced at higher temperatures when the superfluid density is lower. Notice that the DOS near $\omega = 0$ is hardly affected even as the temperature is raised, and therefore we expect that the electronic entropy is only slightly increased due to the longitudinal phase fluctuation as illustrated in Sec. IV.

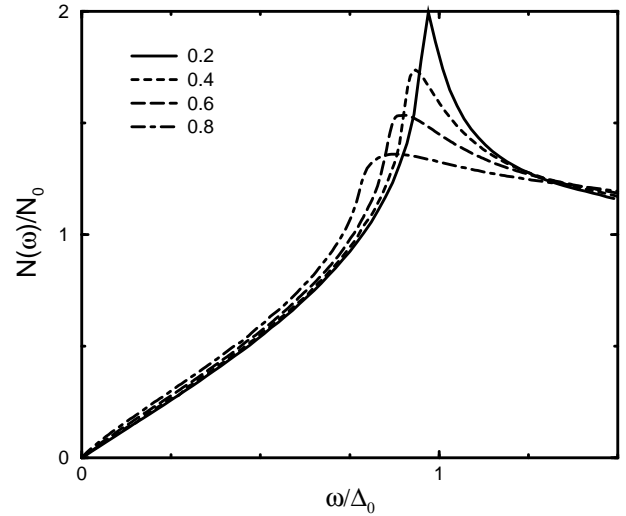


FIG. 5. Density of states in the presence of the longitudinal phase fluctuations at four different temperatures. Here $t = 4mT/n_s(0)$. Above $t = t_{BKT} \approx 0.67$, the vortices are expected to be more important. Here we take $\lambda = \Delta_0/v_F$.

B. Transverse phase fluctuations

Since the two-dimensional superconducting transition is driven by vortex-antivortex pair unbinding, we need to take into account the effect of vortices, especially above the vortex pair unbinding temperature T_{BKT} .¹⁹ We assume that the longitudinal phase fluctuation is less important in this temperature regime and consider only the effect of the vortex distribution or the transverse superfluid velocity (see Appendix A). Using the Dyson equation similar to Sec. III A and neglecting the $\xi_{\mathbf{k}}$ -dependence in the self-energy, from Eqs. (3.6) and (A16) we obtain the following form of the fermion self-energy

$$\hat{\Sigma}_t(\phi, \omega) \approx -\frac{\pi^2 v_F^2}{4\pi^2 K(l^*) \xi_c^2 e^{2l^*}} \int \frac{d^2 q}{(2\pi)^2} \frac{q_\perp^2}{q^2} \frac{1}{q^2 + e^{-2l^*}/\xi_c^2} \frac{1}{q_\parallel^2 v_F^2 + \tilde{\omega}^2 + \tilde{\Delta}^2(\phi)} \times \begin{pmatrix} i\tilde{\omega} & \tilde{\Delta}(\phi) \\ \tilde{\Delta}(\phi) & i\tilde{\omega} \end{pmatrix}, \quad (3.10)$$

where $q^2 = q_\perp^2 + q_\parallel^2$. Again using Eq. (3.8) we can self-consistently calculate $\tilde{\omega}$ and $\tilde{\Delta}$, and subsequently, the Green's function when $T > T_{BKT}$ by analytically continuing the frequency $i\omega \rightarrow \omega + i\eta$.

The ARPES studies of the cuprates show that the quasiparticle spectral function broadens dramatically when passing from the superconducting to the normal state.⁷ How does vortex unbinding contribute to this broadening? In Fig. 6 we show the scattering rate due to the vortices, $1/\tau = \text{Im}\tilde{\omega}$ at $\omega = \Delta_0$ in the three directions ($\phi = 0, \pi/8, \pi/12$). As the temperature is raised from T_{BKT} , $1/\tau$ rapidly increases to a value of order Δ_0 , which is a rather large quantity. This shows that the phase fluctuation is an important ingredient in the broadening of the spectral function. As the temperature is further raised, we expect that the fluctuations in the gap magnitude Δ will further enhance the spectral width, which is beyond the scope of discussion in this paper.

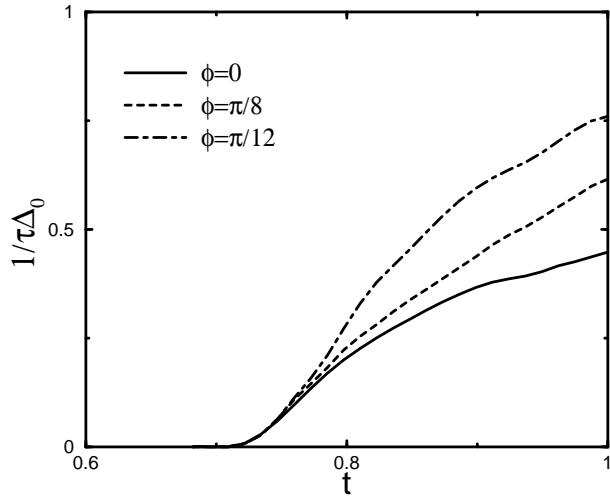


FIG. 6. The scattering rate ($\text{Im}\tilde{\omega}$) as a function of $t = 4mT/n_s(0)$ at $\omega = \Delta_0$ and in the three directions $\phi_1 = 0, \phi_2 = \pi/8, \phi_3 = \pi/12$, in the presence of unbound vortex-antivortex pairs.

So far we have discussed the spectral properties of the *neutral* fermions. Of much interest is the spectral broadening of the physical electrons as revealed by the ARPES data. For instance, in the absence of the interaction term S_I in the action, the Green's function for the physical electrons factors as

$$\langle c_\sigma(\mathbf{x}, \tau) c_\sigma^\dagger(\mathbf{0}, 0) \rangle = \langle e^{i\theta(\mathbf{x}, \tau)/2} e^{-i\theta(\mathbf{0}, 0)/2} \rangle$$

$$\times \langle \psi_\sigma(\mathbf{x}, \tau) \psi_\sigma^\dagger(\mathbf{0}, 0) \rangle. \quad (3.11)$$

We may gain insight into the form of the electron spectral function from Eq. (3.11). Above T_{BKT} , the correlation function $\langle e^{i\theta(\mathbf{x})/2} e^{-i\theta(\mathbf{0})/2} \rangle$ behaves approximately as $e^{-|\mathbf{x}|/4\xi_+}$, where $\xi_+(T)$ is the BKT correlation length,²² and the electron Green's function is roughly

$$\langle c(\mathbf{x}) c^\dagger(\mathbf{0}) \rangle \sim e^{-|\mathbf{x}|/4\xi_+} \mathcal{G}(\mathbf{x}). \quad (3.12)$$

In the low-energy effective theory we consider here, we may think of the quasiparticles as following a quasiclassical trajectory with a Fermi momentum \mathbf{k}_F . Therefore, the leading contribution to the two-point correlation function $\langle c(\mathbf{x}) c^\dagger(\mathbf{0}) \rangle$ comes from the particles with the Fermi momentum \mathbf{k}_F in parallel with the vector $\pm\mathbf{x}$. Then we may treat \mathbf{x} and \mathbf{k}_F as effectively one-dimensional.²³ The one-dimensional Fourier transform of Eq. (3.12) shows that the spectral function of the electrons is additionally broadened by the width $v_F/4\xi_+$ —the electronic spectral width is roughly the sum of $v_F/4\xi_+$ and the spectral width of the neutral fermions.

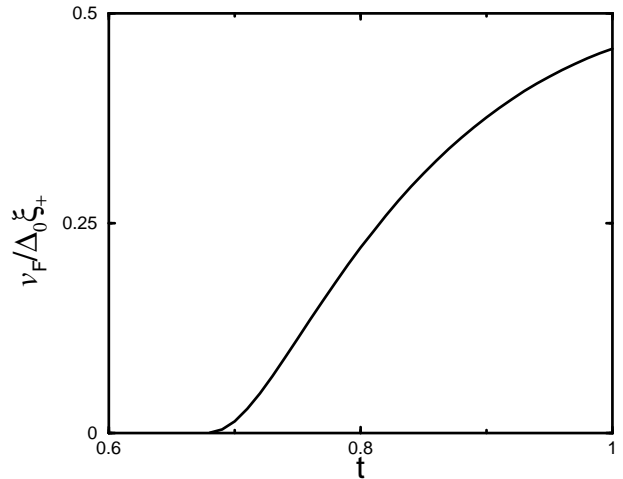


FIG. 7. Inverse of BKT correlation length vs reduced temperature.

As a result of the rapid spectral broadening above T_{BKT} , the single-particle DOS is significantly modified and the singularity at $\omega = \Delta_0$ in the DOS is weakened and broadened. Unlike the case of spectral functions, the neutral fermion DOS coincides with that of physical electrons. Fig. 8 shows the DOS in the maximum gap direction at four different temperatures. When $t > 0.67$, the DOS is rapidly smeared out and the gap is filling in, exhibiting a pseudogap-like behavior.

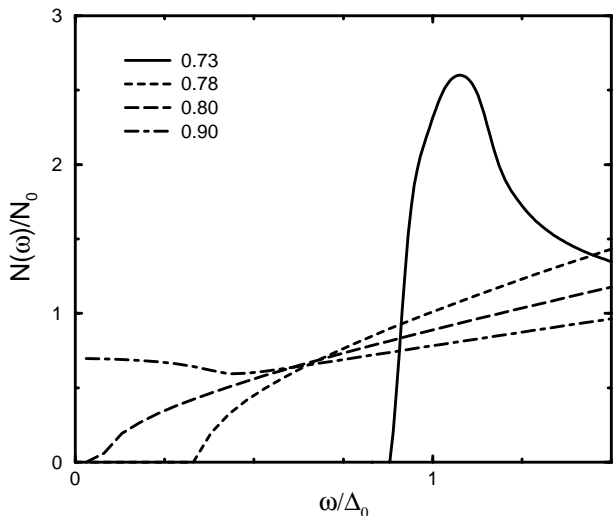


FIG. 8. Density of states at $\phi = 0$ (in the maximum gap direction) at four temperatures above $t_{BKT} = 0.67$ when the unbound vortex-antivortex pairs are taken into account.

IV. THERMODYNAMIC PROPERTIES

Experiments on $Y_{0.8}Ca_{0.2}Ba_2Cu_3O_{7-\delta}$ show that there is a BCS-like discontinuity in the specific heat at optimal doping.⁶ However, in the underdoped regime, the superconducting transitions are marked by weaker and broader peaks in the specific heat. With this puzzling feature in mind, we consider the effect of the phase fluctuations on specific heat in this section.

Before we proceed, we consider one consequence of the pseudogap phenomenon in underdoped cuprates. We can estimate the specific heat change in the presence of the pseudo gap using the BCS mean-field theory;²⁴ the superconducting-normal free energy difference is

$$\Delta F = F_S - F_N = \int_0^{\Delta_s(T)} \frac{d(1/|g|)}{d\Delta_s} \Delta_s^2 d\Delta_s, \quad (4.1)$$

where

$$\frac{1}{|g|} = \frac{mk_F}{2\pi^2} \int_0^{\omega_D} d\xi \frac{\tanh(\sqrt{\xi^2 + \Delta^2(T)}/2T)}{\sqrt{\xi^2 + \Delta^2(T)}}. \quad (4.2)$$

Here g is the BCS pair coupling and Δ_s and Δ are the superconducting gap and the total electronic gap respectively. The ARPES⁷ and STS⁸ data show that the electronic gap evolves smoothly through T_c , from the superconducting gap to the pseudogap. Since $\Delta(T)$ does not rapidly change at T_c and Eq. (4.2) is expressed in terms of $\Delta(T)$ only, $d(1/|g|)/d\Delta_s$ is a very small number and there is no dramatic increase in entropy at T_c . Therefore, we do not expect a BCS-like specific heat jump.

From the above discussion we see that most of the characteristic changes in the specific heat at T_c should come from the order parameter fluctuations. Here we

consider the effect of the phase fluctuations at both $T > T_{BKT}$ and $T < T_{BKT}$. First we consider the electronic entropy change due to the longitudinal phase fluctuations which is more important at $T < T_{BKT}$. From the Green's function and the density of states we obtained in Eq. (3.7) and Eq. (3.9), we may approximately express the entropy as

$$S \approx - \int_0^\infty d\omega N(\omega) \{ f(\omega) \ln f(\omega) + [1 - f(\omega)] \ln [1 - f(\omega)] \}, \quad (4.3)$$

where $N(\omega)$ is the single-particle density of states and $f(x) = 1/(e^{\beta x} + 1)$. We can compare the entropy thus obtained with the mean-field BCS entropy, as illustrated in Fig. 9. We observe that the electronic entropy change is so minute that it may be hardly visible in the specific heat. The small entropy increase is due to the fact that the density of states is affected by the phase fluctuations only when $\omega \approx \Delta_0$ (see Fig. 5); the electronic entropy is insensitive to the longitudinal phase fluctuations.

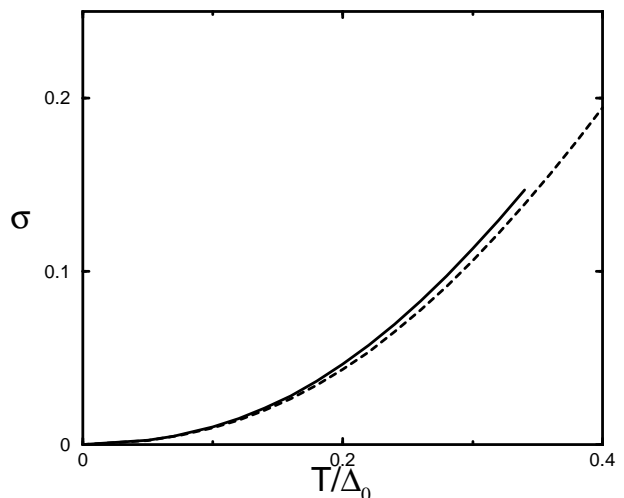


FIG. 9. The reduced electronic entropy $\sigma = (\frac{2\pi E_F}{\Delta_0 k_B}) S$ vs the temperature. σ has the meaning of the entropy in an area of $1/k_F^2$ normalized by the maximum gap energy Δ_0 . The dotted line is the electronic entropy obtained using the d -wave BCS theory, and the solid line is the entropy in the presence of the longitudinal phase fluctuations. Here the case of $n_s(0)/4m = \Delta_0/3$ is illustrated.

Now we turn to the behavior of specific heat in the presence of unbound vortex-antivortex pairs at $T > T_{BKT}$. In the 2D XY model, the vortex-antivortex dissociations cause an unobservable singularity at the transition temperature, followed by a broad bump at a temperature higher than T_{BKT} .²⁵ In conventional superconductors, the bump in the specific heat due to the vortex unbinding may be unobservable—the density of dissociated vortices can be only so large before they saturate the whole sample since the vortex core size is much larger than the electronic mean spacing. However, in the

cuprate superconductors, the vortex core size is only a few times the lattice spacing, so the vortex dissociation may give a sizable contribution to the specific heat. To reduce the theory down to the effective vortex degrees of freedom, we integrate out the fermion fields and express the action in the form in Eq. (A7). Then we can evaluate the specific heat by

$$C = k_B \frac{d}{dT} \left(T^2 \frac{d}{dT} \bar{\mathcal{F}} \right) \quad (4.4)$$

where the reduced free energy is defined as

$$\bar{\mathcal{F}} = \ln \mathcal{Z} = \ln \left(\int \mathcal{D}n e^{-S_v} \right). \quad (4.5)$$

The free energy is a function of the temperature through $K(0)$ and $y(0)$ as defined in Appendix A. We evaluate $\bar{\mathcal{F}}$ following the prescription by Berker and Nelson,²⁵ who computed the specific heat in the 2D XY model. The only difference here is that in our model the superfluid density and the vortex core energy have a temperature dependence whereas in the spin XY model the spin stiffness JT is a constant.

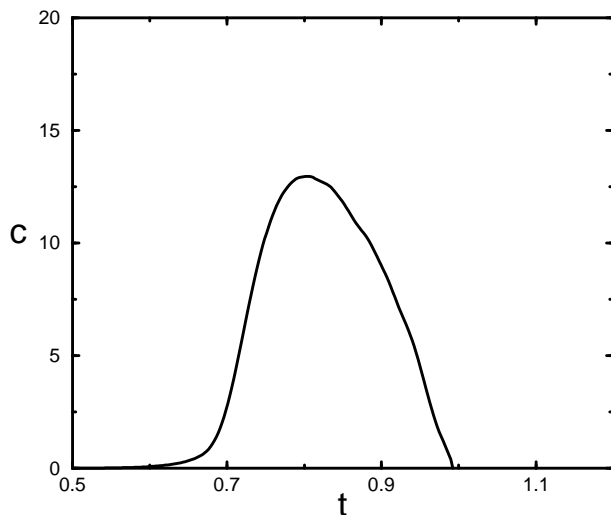


FIG. 10. The reduced heat capacity per area of a vortex core ($c = (\xi_c^2/k_B) C$) vs temperature ($t = 4mT/n_s(0)$). There is a very weak singularity at $t = 0.67$.

The result is shown in Fig. 10. The heat capacity per vortex core area ξ_c^2 is peaked at $t \approx 0.8$ and the peak height about $13k_B$. Now we may cast this result on the electronic length scale. Since $k_F \xi_c \approx 10$ in cuprates, the heat capacity per unit cell of area $1/k_F^2$ is about $0.1k_B$, which is a large number compared to the electronic specific heat. In conventional low- T_c superconductors, there is a factor of 10^{-6} reduction in the peak since $k_F \xi_c \sim 10^3$. The specific heat peak may be practically unobservable in this case. We conclude that if there is a vortex pair unbinding transition in underdoped cuprates, its effect on thermodynamic quantities would be visible, although the

actual specific heat measurement may be complicated by other sources of thermal fluctuations.

V. CONCLUSIONS

The low-energy effective theory which we have applied to the underdoped cuprates is a convenient model which describes a complex many-body system (whose microscopic details are unknown) in terms of a few macroscopic parameters such as the superfluid density, effective mass, and the magnitude of the superconducting gap. Utilizing this phenomenological theory, we are able to calculate the spectral properties in the presence of phase fluctuations without regard to the microscopic details. By assuming a robust quasiparticle gap and a small superfluid density, as appropriate for the underdoped cuprates, we found that the vortex pair unbinding transition causes pronounced effects on the single-particle properties: (i) The peak in the spectral function is dramatically broadened as the temperature is raised through T_{BKT} ; (ii) The density of states is widely smeared out at $T > T_{BKT}$, significantly deviating from the usual superconducting state although the gap magnitude is robust. These two features are reminiscent of the pseudogap behavior in underdoped cuprates, as observed in the ARPES⁷ and STS⁸ experiments. It is remarkable that we can reproduce a few of the pseudogap-like properties by including only the phase degree of freedom. This indicates that along with the fluctuations in the order parameter amplitude, the phase fluctuations may be an essential ingredient in the pseudogap phenomena. For instance, phase fluctuations may better explain the fact that the superconducting gap nodes evolve into extended gapless Fermi arcs in the pseudogap phase since the phase fluctuations are more significant near the nodes (Fig. 6). The amplitude fluctuations alone may not be sufficient to explain this.²⁶

The role of phase fluctuations in the pseudogap regime has recently been explored in several approaches which bear some similarity to ours. As mentioned in Sec. II, Franz and Millis¹⁷ have also studied the effect of classical phase fluctuations on the spectroscopic properties of the underdoped cuprates, by coupling the d -wave quasiparticles to the fluctuating supercurrents due to unbound vortex-antivortex pairs. While our approach to treating this coupling is quite different from the approach of Franz and Millis, our conclusions are similar—that transverse phase fluctuations are important in determining the spectral properties above T_c . On a different tack, Balents, Fisher, and Nayak²⁷ have recently proposed a zero-temperature “nodal liquid theory” in which there is a transition between the superconducting phase and the nodal liquid (tentatively identified as the ground state of the pseudogap regime) which is driven by *quantum* fluctuations of the order-parameter phase. The properties of this model at non-zero temperatures have yet to be investigated.

Before closing we should note that our interpretation of the pseudogap regime as the remnant of a superconducting phase which has been destroyed by phase fluctuations is not without criticism. Geshkenbein *et al.*²⁸ and Randeria⁹ have argued that the fluctuation effects should be significant over a much wider temperature range than is observed experimentally, and that strong pairing correlations (beyond BCS theory) need to be incorporated into any model of the pseudogap regime. A completely different explanation of the pseudogap behavior has been proposed by Lee and Wen,²¹ who argue that the superconducting phase is destroyed by the thermal excitation of nodal quasiparticles, which quenches the superfluid density while retaining the quasiparticle gap. Finally, we have neglected the Coulomb interaction in our model; including it would presumably suppress the longitudinal phase fluctuations while leaving the transverse fluctuations unaffected.¹⁷ All of these criticisms merit further investigation in a more detailed study of the pseudogap phenomenon.

ACKNOWLEDGMENTS

We would like to thank Mohit Randeria for many helpful discussions on the phenomenology of the underdoped cuprates; Marcel Franz and Wilhelm Zwerger for their helpful comments on the manuscript; and Matthew Fisher for pointing out possible difficulties with the gauge transformation in the presence of vortices. This work was supported by NSF grant DMR 96-28926 and by the National High Magnetic Field Laboratory.

APPENDIX A: LONGITUDINAL AND TRANSVERSE FLUCTUATIONS OF THE SUPERFLUID VELOCITY

For the sake of completeness, in this Appendix we have collected together some of the important results regarding the Berezinskii-Kosterlitz-Thouless (BKT) transition¹⁹ which pertain to our calculation of the fermion self-energy. A more detailed discussion can be found in Ref. 29. First, we resolve the phase field into longitudinal (spin wave) and transverse (vortex) components. This is done by writing $\theta = \theta_a + \theta_v$, with θ_a the analytic spin-wave contribution and θ_v the singular vortex contribution. The superfluid velocity can then be decomposed as $\mathbf{v}_s = (1/2m)\nabla\theta = \mathbf{v}_s^l + \mathbf{v}_s^t$, with $\mathbf{v}_s^l = (1/2m)\nabla\theta_a$ and $\mathbf{v}_s^t = (1/2m)\nabla\theta_v$, such that $\nabla \times \mathbf{v}_s^l = 0$ and $\nabla \cdot \mathbf{v}_s^t = 0$. The classical phase action then becomes

$$\begin{aligned} S &= \frac{mn_s(T)}{2T} \int d^2x v_s^2 \\ &= \frac{mn_s(T)}{2T} \int d^2x [(v_s^l)^2 + (v_s^t)^2], \end{aligned} \quad (\text{A1})$$

since the cross term is zero as shown below.

The curl of the transverse component is the total vorticity; for singly quantized vortices with circulation $\pm 2\pi\hbar/2m$, this can be written as

$$\nabla \times \mathbf{v}_s^t = \frac{2\pi}{2m} n(\mathbf{x}) \hat{z}, \quad (\text{A2})$$

where the vortex density $n(\mathbf{x})$ is

$$n(\mathbf{x}) = \sum_i q_i \delta(\mathbf{x} - \mathbf{x}_i), \quad (\text{A3})$$

with vortices at positions $\{\mathbf{x}_i\}$ and with vortex ‘‘charges’’ $q_i = \pm 1$ (here we consider only neutral vortex configurations such that $\sum_i q_i = 0$). Using the fact that \mathbf{v}_s^t is transverse,

$$\mathbf{v}_s^t(\mathbf{x}) = \nabla \times \int d^2x' G(\mathbf{x} - \mathbf{x}') \frac{2\pi}{2m} n(\mathbf{x}') \hat{z}, \quad (\text{A4})$$

where $\nabla^2 G = -\delta(\mathbf{x} - \mathbf{x}')$; Fourier transforming,

$$\mathbf{v}_s^t(\mathbf{q}) = i \frac{\mathbf{q} \times \hat{z}}{q^2} \frac{2\pi}{2m} n(\mathbf{q}). \quad (\text{A5})$$

The analogous expression for the longitudinal component is

$$\mathbf{v}_s^l(\mathbf{q}) = \frac{i\mathbf{q}}{2m} \theta_a(\mathbf{q}). \quad (\text{A6})$$

It is easy to verify that the cross term $\mathbf{v}_s^t(\mathbf{q}) \cdot \mathbf{v}_s^l(\mathbf{q})$ in Eq. (A1) is zero. The final expression for the vortex contribution to the classical phase action is obtained by substituting Eq. (A5) into Eq. (A1):

$$\begin{aligned} S_v &= \pi K(0) \int \int_{|\mathbf{x}-\mathbf{x}'|>\xi_c} d^2x d^2x' n(\mathbf{x}) n(\mathbf{x}') \ln(|\mathbf{x} - \mathbf{x}'|/\xi_c) \\ &\quad + \ln y(0) \int d^2x n^2(\mathbf{x}) \\ &= \frac{1}{2} \sum_{\mathbf{q}} \left\{ \frac{4\pi^2 K(0)}{q^2} - 8\pi \xi_c^2 \ln [y(0)] \right\} n(\mathbf{q}) n(-\mathbf{q}), \end{aligned} \quad (\text{A7})$$

where $K(0) = n_s(T)/4mT$ is the bare spin stiffness, $y(0) = \exp(-\mathcal{E}_c/4\pi T)$ is the bare fugacity with $\mathcal{E}_c = TK(0) \ln \kappa$ the vortex core energy, $\xi_c \sim v_F/\Delta_0$ is the vortex core size, and κ is the ratio of the magnetic penetration depth to the coherence length.

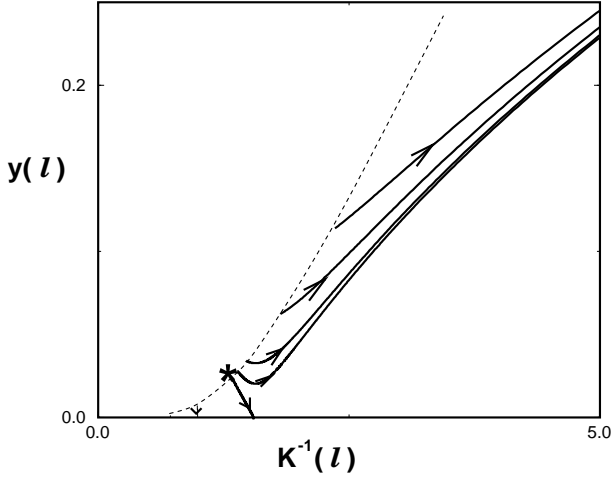


FIG. 11. The RG flow of $(K^{-1}(l), y(l))$. The dashed curve is the locus of initial values $(K^{-1}(0), y(0))$. The asterisk (*) marks the vortex pair unbinding transition temperature (T_{BKT}) which in this model corresponds to $4mT_{BKT}/n_s(0) \approx 0.67$. Above this transition temperature, $(K^{-1}(0), y(0))$ rides on the outgoing curves and $(K^{-1}(l), y(l))$ values diverge in the $l \rightarrow \infty$ limit.

In this model there is a critical temperature T_{BKT} above which the two-dimensional quasi-long-range order is destroyed by thermal fluctuations. At $T < T_{BKT}$, the vortices are bound into neutral pairs (when there is no external magnetic field), and the superfluid density is non-zero. In this temperature regime, consideration of the soft longitudinal phase fluctuation θ_a is sufficient. When $T > T_{BKT}$, the bound pairs of vortices dissociate and free vortices proliferate as the temperature is raised, driving the superfluid density to zero. This picture is made quantitative using the RG flow equations¹⁹ for the coupling constants $(K(l), y(l))$ at the length scale e^l (see Fig. 11):

$$\begin{aligned} \frac{dK^{-1}(l)}{dl} &= 4\pi^3 y^2(l), \\ \frac{dy(l)}{dl} &= [2 - \pi K(l)]y(l). \end{aligned} \quad (\text{A8})$$

To calculate the fermion self-energy we need the vortex-vortex correlation function $\langle n(\mathbf{q})n(-\mathbf{q}) \rangle \equiv \Gamma_2(\mathbf{q}, K(0), y(0))$, which can be calculated approximately using the Debye-Hückel theory developed by Halperin and Nelson.³⁰ To implement this, we first note that under scale transformations the correlation function scales as

$$\Gamma_2(\mathbf{q}, K(0), y(0)) = e^{-2l} \Gamma_2(e^l \mathbf{q}, K(l), y(l)). \quad (\text{A9})$$

Now we integrate the RG flow equations out to a length scale l^* where the density of free vortices is high; at this scale we may integrate over the coarse-grained vortex density rather than the individual vortex coordinates (the Debye-Hückel approximation). Since the classical

phase action, Eq. (A7), is quadratic in the vortex density, the correlation function is

$$\Gamma_2(\mathbf{q}, K(0), y(0)) = \frac{e^{-2l^*}}{4\pi^2 K(l^*) / (e^{l^*} q)^2 - 8\pi \xi_c^2 \ln y(l^*)}. \quad (\text{A10})$$

If we choose l^* such that

$$4\pi^2 K(l^*) \xi_c^2 = -8\pi \xi_c^2 \ln y(l^*), \quad (\text{A11})$$

then the correlation function takes the particularly simple form

$$\Gamma_2(\mathbf{q}, K(0), y(0)) = \frac{1}{4\pi^2 K(l^*)} \frac{1}{1/q^2 + \xi_c^2 e^{2l^*}}. \quad (\text{A12})$$

Both l^* and $K(l^*)$ are determined from a numerical integration of the RG equations, Eq. (A8).

Using these results we can calculate the velocity-velocity correlation function for $T > T_{BKT}$,

$$\begin{aligned} \langle v_s^\alpha(\mathbf{q}) v_s^\beta(-\mathbf{q}) \rangle &= C_l(\mathbf{q}) \hat{q}_\alpha \hat{q}_\beta \\ &+ C_t(\mathbf{q}) (\delta_{\alpha\beta} - \hat{q}_\alpha \hat{q}_\beta), \end{aligned} \quad (\text{A13})$$

where the longitudinal component is

$$\begin{aligned} C_l(\mathbf{q}) &= \frac{q^2}{4m} \langle \theta_a(\mathbf{q}) \theta_a(-\mathbf{q}) \rangle \\ &= \frac{T}{4m^2 n_s(T)}, \end{aligned} \quad (\text{A14})$$

and the transverse component is

$$\begin{aligned} C_t(\mathbf{q}) &= \frac{\pi^2}{m^2} \frac{\langle n(\mathbf{q}) n(-\mathbf{q}) \rangle}{q^2} \\ &= \frac{1}{4m^2 K(l^*)} \frac{1}{1 + \xi_c^2 e^{2l^*} q^2}. \end{aligned} \quad (\text{A15})$$

APPENDIX B: DETAILS OF THE CALCULATION OF THE SELF-ENERGY

In this Appendix we provide some of the details of the calculation of the self energy in Eqs. (3.7) and (3.8).

Near the Fermi surface, neglecting the $\xi_{\mathbf{k}}$ -dependence in $\Sigma(\mathbf{k}, \omega)$,

$$\begin{aligned} \hat{G}^{-1}(\mathbf{k}, \omega) &= \begin{pmatrix} i\tilde{\omega} - \xi_{\mathbf{k}} & -\tilde{\Delta}(\phi) \\ -\tilde{\Delta}(\phi) & i\tilde{\omega} + \xi_{\mathbf{k}} \end{pmatrix} \\ &= \begin{pmatrix} i\omega - \xi_{\mathbf{k}} & -\Delta(\phi) \\ -\Delta(\phi) & i\omega + \xi_{\mathbf{k}} \end{pmatrix} - \hat{\Sigma}(\phi, \omega), \end{aligned} \quad (\text{B1})$$

where ϕ is the angle on the Fermi surface. From Eq. (3.4), when $|\mathbf{k}| = k_F$,

$$\begin{aligned} \hat{\Sigma}_l(\phi, \omega) &\approx - \sum_{\mathbf{q}} \left[m \mathbf{v}_F(\mathbf{k}) \cdot \hat{q} \right]^2 C_l(\mathbf{q}) \begin{pmatrix} i\tilde{\omega} + \delta\xi_{\mathbf{q}} & \tilde{\Delta}(\phi) \\ \tilde{\Delta}(\phi) & i\tilde{\omega} - \delta\xi_{\mathbf{q}} \end{pmatrix} \\ &\times \frac{1}{\tilde{\omega}^2 + (\delta\xi_{\mathbf{q}})^2 + \tilde{\Delta}^2(\phi)}, \end{aligned} \quad (\text{B2})$$

where $\delta\xi_{\mathbf{q}} = \mathbf{v}_F(\mathbf{k}) \cdot \mathbf{q}$. Now, using the integral

$$\begin{aligned} & \int dx dy \frac{x^2}{x^2 + y^2} \frac{1}{x^2 + a^2} \\ & \approx \int_{-\lambda}^{\lambda} dx \int_{-\infty}^{\infty} dy \frac{x^2}{x^2 + y^2} \frac{1}{x^2 + a^2} \\ & = \pi \ln \left(\frac{\lambda^2 + a^2}{a^2} \right), \end{aligned} \quad (\text{B3})$$

we obtain Eq. (3.7).

* Electronic mail: hjk@phys.ufl.edu.

** Electronic mail: dorsey@phys.ufl.edu.

¹ M. Takigawa *et al.*, Phys. Rev. B **43**, 247 (1991); G. V. M. Williams *et al.*, Phys. Rev. Lett. **78**, 721 (1997).

² J.M. Tranquada *et al.*, Phys. Rev. B **46**, 5561 (1992).

³ S.L. Cooper *et al.*, Phys. Rev. B **40**, 11 358 (1989); J. Orenstein *et al.*, Phys. Rev. B **42**, 6342 (1990); L.D. Rotter *et al.*, Phys. Rev. Lett. **67**, 2741 (1991); S.L. Cooper *et al.*, Phys. Rev. B **47**, 8233 (1993); C.C. Homes *et al.*, Phys. Rev. Lett. **71**, 1645 (1993); A. V. Puchkov *et al.*, Phys. Rev. Lett. **77**, 1853 (1996); D. N. Basov *et al.*, Phys. Rev. Lett. **77**, 4090 (1996).

⁴ B. Bucher *et al.*, Phys. Rev. Lett. **70**, 2012 (1993); T. Ito, K. Takenaka, and S. Uchida, Phys. Rev. Lett. **70**, 3995 (1993); T. Watanabe, T. Fujii, and A. Matsuda, Phys. Rev. Lett. **79**, 2113 (1997).

⁵ R. Nemetschek *et al.*, Phys. Rev. Lett. **78**, 4837 (1997); G. Blumberg *et al.*, Science **278**, 1427 (1997).

⁶ J. W. Loram *et al.*, Phys. Rev. Lett. **71**, 1740 (1993); Physica C **282-287**, 1405 (1997).

⁷ H. Ding *et al.*, Nature **382**, 51 (1996); M. R. Norman, M. Randeria, H. Ding and J. C. Campuzano, Phys. Rev. B **57**, R11093 (1998); H. Ding *et al.*, cond-mat/9712100.

⁸ Ch. Renner *et al.*, Phys. Rev. Lett. **80**, 149 (1998); A. K. Gupta and K.-W. Ng, Phys. Rev. B **58**, R8901 (1998).

⁹ For an overview of the experimental results and their interpretation, see M. Randeria, cond-mat/9710223.

¹⁰ V. J. Emery and S. A. Kivelson, Nature **374**, 434 (1995); cond-mat/9710059.

¹¹ Y. J. Uemura *et al.*, Phys. Rev. Lett. **62**, 2317 (1989).

¹² T. Jacobs *et al.*, Phys. Rev. Lett. **75**, 4516 (1995); C. Panagopoulos, J. R. Cooper and T. Xiang, Phys. Rev. Lett. **79**, 2320 (1998).

¹³ A. L. Fetter and J. D. Walecka, *Quantum Theory of Many-Particle Systems* (McGraw-Hill, San Francisco, 1971), pp. 459–460.

¹⁴ It has been pointed out to us (M.P.A. Fisher, private communication) that in the presence of unbound, singly quantized vortices this gauge transformation is singular, and therefore multi-valued. One can in principle remedy this difficulty by defining branch cuts in the two dimensional plane which terminate on the vortices; however, in practice it is unclear how one would incorporate this cut structure

into a perturbative many-body calculation, such as the one which we develop in this work. We leave this as an unresolved issue which deserves further study.

¹⁵ R. Shankar, Physica A **177**, 530 (1991); Rev. Mod. Phys. **66**, 129 (1994). A similar idea was used in A. F. Andreev, Zh. Eksp. Theor. Fiz. **46**, 1823 (1964) [Sov. Phys. JETP **19**, 1228 (1964)].

¹⁶ S. Stintzing and W. Zwerger, Phys. Rev. B **56**, 9004 (1997) estimate that $k_F \xi_0 \sim 5 - 8$, using a Ginzburg-Landau theory which describes the crossover from BCS theory to Bose condensation.

¹⁷ M. Franz and A.J. Millis, cond-mat/9805401.

¹⁸ T.V. Ramakrishnan, Physica Scripta **T27**, 24 (1989).

¹⁹ V. L. Berezinskii, Zh. Eksp. Theor. Fiz. **59**, 907 (1970) [Sov. Phys. JETP **32**, 493 (1971)]; J. M. Kosterlitz and D. J. Thouless, J. Phys. C **6**, 1181 (1973).

²⁰ J. Corson *et al.*, cond-mat/9810280.

²¹ P. A. Lee and X.-G. Wen, Phys. Rev. Lett. **78**, 4111 (1997).

²² P. Minnhagen, Rev. Mod. Phys. **59**, 1001 (1987).

²³ H.-J. Kwon, A. Houghton, and J. B. Marston, Phys. Rev. B **52**, 8002 (1995).

²⁴ A. A. Abrikosov, L. P. Gorkov, and I. E. Dzyaloshinski, *Methods of Quantum Field Theory in Statistical Physics* (Dover, New York, 1963).

²⁵ A. N. Berker and D. R. Nelson, Phys. Rev. B **19**, 2488 (1979).

²⁶ H.-J. Kwon, cond-mat/9811059.

²⁷ L. Balents, M.P.A. Fisher, and C. Nayak, Int. J. Mod. Phys. B **12**, 1033 (1998).

²⁸ V.B. Geshkenbein, L.B. Ioffe, and A.I. Larkin, Phys. Rev. B **55**, 3173 (1997); A.J. Millis, S.M. Girvin, L.B. Ioffe, and A.I. Larkin, cond-mat/9709222.

²⁹ P.M. Chaikin and T.C. Lubensky, *Principles of Condensed Matter Physics* (Cambridge University Press, Cambridge, 1995), Sec. 9.4.

³⁰ B. I. Halperin and D. R. Nelson, J. Low Temp. Phys. **36**, 599 (1979).